

Two-body transients in coupled atomic-molecular BECs

Pascal Naidon¹, Eite Tiesinga^{1,2} and Paul S. Julienne^{1,2}

¹Atomic Physics Division and ²Joint Quantum Institute
National Institute of Standards and Technology and University of Maryland,
100 Bureau Drive Stop 8423, Gaithersburg, Maryland 20899-8423, USA

We discuss the dynamics of an atomic Bose-Einstein condensate when pairs of atoms are converted into molecules by single-color photoassociation. Three main regimes are found and it is shown that they can be understood on the basis of time-dependent two-body theory. In particular, the so-called rogue dissociation regime [Phys. Rev. Lett., **88**, 090403 (2002)], which has a density-dependent limit on the photoassociation rate, is identified with a transient regime of the two-atom dynamics exhibiting universal properties. Finally, we illustrate how these regimes could be explored by photoassociating condensates of alkaline-earth atoms.

The conversion of atom pairs into molecules, using either Feshbach resonances [1] or photoassociation [2], serves as a tool to probe the many-body properties of ultracold gases [3]. In particular, photoassociation, the process of associating atoms with a resonant laser light, was recently used to observe pair correlation in a one-dimensional Bose gas [4] and the crossover between Bose-Einstein condensate (BEC) and Bardeen-Cooper-Schrieffer (BCS) superfluid [5]. Conversely, it can be used to reach new regimes. Many-body theories have suggested the coherent conversion of an atomic BEC into one of molecules [6, 7], macroscopic superposition [8], and production of correlated atom pairs at high laser intensity [9, 10, 11]. Several experiments have made the first steps in these directions [12, 13, 14, 15], but have been limited by inherent losses or insufficient laser power. Reference [11] identified three regimes of photoassociation as a function of loss and laser intensity. The intriguing density dependence of the regime boundaries suggested that they are associated to many-body effects.

In this letter, we first apply time-dependent two-body theory to photoassociation with a single continuous laser and distinguish three transient regimes. We then show how these transients explain the previously identified regimes in the many-body theories.

For two atoms of mass M interacting with a resonant laser, photoassociation is described by two equations coupling a scattering and a molecular channel [16],

$$i\hbar\dot{\phi}(\vec{r}) = \left(-\frac{\hbar^2}{M}\nabla^2 + U(r) \right) \phi(\vec{r}) + W(\vec{r})\phi_m(\vec{r})$$

$$i\hbar\dot{\phi}_m(\vec{r}) = \left(-\frac{\hbar^2}{M}\nabla^2 + U_m(r) - i\frac{\gamma}{2} \right) \phi_m(\vec{r}) + W(\vec{r})\phi(\vec{r}),$$

where \vec{r} is the relative separation of the two atoms, $\phi(\vec{r})$ and $\phi_m(\vec{r})$ are the components of the relative motion wave function for the scattering and molecular channels, U and U_m are the interaction potentials in each channel, γ is the spontaneous emission rate from the molecular channel (we assume that decayed molecules are lost from the system), and W couples the two channels. W is proportional to the square root of the laser intensity. We expand $|\phi\rangle$ and $|\phi_m\rangle$ in the bases of eigenstates of $-\frac{\hbar^2}{M}\nabla^2 + U$ and $-\frac{\hbar^2}{M}\nabla^2 + U_m$, re-

spectively, and assume that only the scattering eigenstates $|\varphi_{\vec{k}}\rangle$ (indexed by wave vector \vec{k}) are relevant in the scattering channel, and that a single bound eigenstate $|\varphi_m\rangle$ is resonant in the molecular channel. Choosing $\langle\varphi_m|\varphi_m\rangle = 1$ and $\langle\varphi_{\vec{k}}|\varphi_{\vec{p}}\rangle = (2\pi)^3\delta^3(\vec{k} - \vec{p})$, one obtains

$$i\hbar\dot{C}_{\vec{k}}(t) = E_k C_{\vec{k}}(t) + w_{\vec{k}} C_m(t) \quad (1)$$

$$i\hbar\dot{C}_m(t) = (\Delta - i\gamma/2) C_m(t) + \int \frac{d^3\vec{k}}{(2\pi)^3} w_{\vec{k}} C_{\vec{k}}(t), \quad (2)$$

where $C_{\vec{k}}$ and C_m are the amplitudes in states $|\varphi_{\vec{k}}\rangle$ and $|\varphi_m\rangle$, $E_k = \hbar^2 k^2 / M$, Δ is the resonant bound state energy with respect to the scattering threshold (which can be adjusted by tuning the laser frequency), and $w_{\vec{k}} = \langle\varphi_m|W|\varphi_{\vec{k}}\rangle$ are the coupling matrix elements. According to Wigner's threshold laws, $w_{\vec{k}}$ goes to a constant w for low $k \ll 1/|r_c|$, where r_c is the largest of the extent of the molecule, the van der Waals length [2], or the scattering length a associated with U .

In ultracold gases, atoms collide at nearly zero energy. For the stationary solution at zero energy, $C_{\vec{k}}$ goes to $-4\pi A/k^2$ for low k , where A is the optically-induced complex scattering length [16, 17] given by $4\pi\hbar^2 A = -M|w|^2/(\Delta - \Delta' - i\gamma/2)$ and the light shift $\Delta' = \int \frac{d^3\vec{k}}{(2\pi)^3} \frac{|w_{\vec{k}}|^2}{E_k}$. The imaginary part of A is related to the loss rate coefficient

$$K = -\frac{8\pi\hbar}{M} \text{Im} A = \frac{2}{\hbar} \text{Im} \frac{|w|^2}{\Delta - \Delta' - i\gamma/2}, \quad (3)$$

which corresponds to the number of atoms lost per unit of time and volume due to photoassociation to the excited state and subsequent decay by spontaneous emission. From kinetic theory the density ρ of remaining atoms in a thermal gas is expected to follow the rate equation

$$\dot{\rho} = -K\rho^2. \quad (4)$$

We now take into account the fact that the laser is turned on at $t = 0$, creating a strong perturbation to the two-body system. As a result, transient regimes appear before the stationary solution is reached. Initially, the two atoms are in the scattering channel with nearly zero collision energy, *i.e.*

$C_{\vec{k}} = (2\pi)^3 \delta^3(\vec{k})$ and $C_m = 0$ at $t = 0$. For $t > 0$ we choose to decompose $C_{\vec{k}}(t)$ as follows

$$C_{\vec{k}}(t) = (2\pi)^3 \delta^3(\vec{k}) + C_{\vec{k}}^{ad}(t) + C_{\vec{k}}^{dyn}(t), \quad (5)$$

where $C_{\vec{k}}^{ad}(t) = -\frac{w_{\vec{k}}}{E_{\vec{k}}} C_m(t)$ is the adiabatic response to the turn-on of the laser (obtained by setting $\dot{C}_{\vec{k}} = 0$ in Eq. (1)), and $C_{\vec{k}}^{dyn}(t)$ is the dynamic response. Solving for $C_{\vec{k}}^{dyn}$ from Eqs. (1) and (5) and inserting it into Eq. (2), we obtain

$$i\hbar \dot{C}_m(t) = \left(\Delta - \Delta' - i\frac{\gamma}{2} \right) C_m(t) + w \left[1 + w \frac{1-i}{2\hbar} \left(\frac{M}{2\pi\hbar} \right)^{3/2} \int_0^t \frac{\dot{C}_m(\tau)}{\sqrt{t-\tau}} d\tau \right],$$

where we have set $w_{\vec{k}} = w$, which is valid for $t \gg t_c$, $t_c = Mr_c^2/\hbar$ being in most cases a very short time scale on the order of 10 ns. We then assume that $\dot{C}_m(t)$ is localized at short times, which leads to the Ansatz $\int_0^t d\tau \dot{C}_m(\tau)/\sqrt{t-\tau} = \alpha C_m(t)/\sqrt{t}$, where α is to be determined, and we approximate $i\hbar \dot{C}_m(t)$ by the short-time expression $i\hbar C_m(t)/t$. This leads to

$$C_m(t) = \frac{-w}{\left(\Delta - \Delta' - i\frac{\gamma}{2} \right) + S(t) - \frac{i\hbar}{t}}, \quad (6)$$

where $S(t) = \frac{1-i}{2} \frac{\hbar}{\sqrt{t_w t}}$ and $\frac{i\hbar}{t}$ are time-dependent shifts and broadenings of the molecular level, and $t_w = \frac{1}{\alpha^2} \left(\frac{\hbar}{M} \right)^3 \left(\frac{\hbar}{w} \right)^4$. In the limit of large $S(t)$, one has $C_m(t) = -\frac{2w}{\hbar(1-i)} \sqrt{t_w t}$ which justifies that $\dot{C}_m(t) \propto t^{-1/2}$ is localized at short times and yields $\alpha = \pi/2$. For small $S(t)$, our Ansatz may not hold but this has little consequence precisely because $S(t)$ is small.

We can now calculate an instantaneous rate coefficient, based on the time variation of the population $\int_{\vec{k} \approx 0} \frac{d^3 \vec{k}}{(2\pi)^3} |C_{\vec{k}}|^2$ in the initial state. This population is always infinite, because we started from a state which is not normalizable over an infinite volume. However, from Eq. (1), its time derivative has a finite value, which we identify as minus the instantaneous rate coefficient, $-K(t)$. Using Eq. (5), we can simplify it to

$$K(t) = -\frac{2}{\hbar} \text{Im}(w^* C_m(t)). \quad (7)$$

Depending on the relative strength of the terms in the denominator of Eq. (6), this coefficient goes through three subsequent regimes illustrated in Fig. 1: linear (a), square root (b), and constant with time (c). Namely,

$$(a) \quad K(t) = \frac{2}{\hbar} \frac{|w|^2}{\hbar} t, \quad \text{for } t_c \ll t \ll t_w \quad (8)$$

$$(b) \quad K(t) = 4/\pi (h/M)^{3/2} \sqrt{t}, \quad \text{for } t_w \ll t \ll t_A \quad (9)$$

$$(c) \quad K(t) = \frac{2}{\hbar} \frac{\text{Im} \frac{|w|^2}{\Delta - \Delta' - i\gamma/2}}{\hbar}, \quad \text{for } t_A \ll t. \quad (10)$$

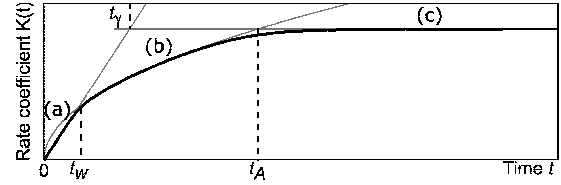


Figure 1: Schematic evolution of the rate coefficient (thick black curve) showing the three regimes (a) (b), and (c) at sufficiently high laser intensity ($t_w \ll t_A$). The grey curves correspond to the limiting expressions (8-10). In particular, the parabolic curve associated with Eq. (9) is a universal upper limit to the rate coefficient.

where $t_A = \alpha^2 \frac{2M}{\hbar} |A|^2$. Note that $t_w \ll t_A$ only for high laser intensity. If $t_w \gtrsim t_A$, regime (a) occurs for $t \ll t_\gamma$ and regime (c) occurs for $t \gg t_\gamma$, where $t_\gamma = \hbar/\sqrt{(\Delta - \Delta')^2 + (\gamma/2)^2}$.

Photoassociation converts the initial state into the molecular state and the loss rate coefficient grows linearly in regime (a). In regime (b) the laser also drives molecules back to the atom-pair continuum. This broadens the resonance and the loss rate coefficient still increases but more slowly. Finally, in regime (c) the molecules start decaying spontaneously, and the rate coefficient reaches its steady-state maximal value, which is the rate coefficient Eq. (3) obtained from the stationary solution.

The atomic density is expected to follow Eq. (4) with the time-dependent rate coefficient (7). Whether the transient regimes (a) and (b) are observable depends on whether an appreciable fraction of the density is photoassociated over these time scales. Let us define the depletion time t_ρ for which an appreciable fraction is depleted, *i.e.* $K(t_\rho)\rho_0 t_\rho \approx 1$, where ρ_0 is the initial density. Three cases are possible. If $t_A, t_\gamma \ll t_\rho$, then only the final constant rate coefficient is relevant. If $t_w \ll t_\rho \ll t_A$, then the first regime to lead to observable losses is regime (b). If $t_\rho \ll t_w, t_\gamma$, then the only relevant regime is (a).

Interestingly, when regime (b) dominates, the molecular amplitude vanishes and the system has a universal behavior. The loss rate (9) and the atom pair distribution

$$C_{\vec{k}}(t) = (2\pi)^3 \delta^3(\vec{k}) + \frac{4}{k^2} \sqrt{\frac{2i\hbar t}{M}} - \frac{4\pi i}{k^3} \text{Erf}\left(k \sqrt{\frac{\hbar t}{iM}}\right) e^{-ik^2 \frac{\hbar t}{M}}$$

do not depend on the microscopic details of the transition, but just on the mass of the species. Here, Erf denotes the error function. The condition $t_w \ll t_\rho \ll t_A$, needed for the observation of this regime, is equivalent to

$$\rho_0^{1/3} |A| \gg (2\pi)^{-2/3} \quad \text{and} \quad \rho_0^{1/3} B \ll (2\pi)^{-2/3} \quad (11)$$

where the length B is $8 \left(\frac{\hbar^2}{Mw} \right)^2$. Finite temperature adds the condition that $K(t_\rho)$ be smaller than the unitarity limit $\frac{\hbar}{M} \lambda$, where λ is the de Broglie wavelength. It fortuitously coincides with the condensation condition for bosons $\rho \lambda^3 \gtrsim 1$ [9, 12].

We now turn to a many-body description. Photoassociation in a uniform BEC can be described (up to first order in

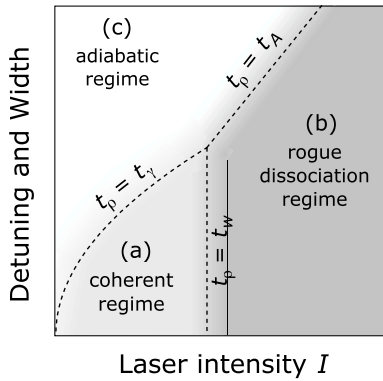


Figure 2: Regimes of photoassociation in a BEC as a function of the “detuning and width” $\sqrt{(\Delta - \Delta')^2 + (\gamma/2)^2}$ and the laser intensity I , for a fixed density. The boundaries are indicated by dashed lines and equalities of time scales defined in the text.

a cumulant expansion [18]) by the three equations [10, 11]

$$\begin{aligned}
 i\hbar\dot{\Psi} &= \Psi^* \int \left(U(r)\Phi(\vec{r}) + W(r, t)\Phi_m(\vec{r}) \right) d^3r \\
 i\hbar\dot{\Phi}(\vec{r}) &= \left(-\frac{\hbar^2}{M}\nabla^2 + U(r) \right) \Phi(\vec{r}) + W(\vec{r})\Phi_m(\vec{r}) + 2i\hbar\Psi\dot{\Psi} \\
 i\hbar\dot{\Phi}_m(\vec{r}) &= \left(-\frac{\hbar^2}{M}\nabla^2 + U_m(r) - i\gamma/2 \right) \Phi_m(\vec{r}) + W(\vec{r})\Phi(\vec{r})
 \end{aligned}$$

where Ψ is the condensate wavefunction (here a complex number), and $\Phi(\vec{r})$ and $\Phi_m(\vec{r})$ are the pair wavefunctions in the scattering and molecular channels. Higher-order cumulants (such as the normal density of noncondensate atoms [19]) contribute significantly only for $t \gtrsim t_\rho$, and do not change the dynamics up to 10 μs in the examples to follow. Inelastic collisions [20], not included here, do not affect the atomic BEC during this time frame for typical rate coefficients $\sim 10^{-10} \text{ cm}^3 \text{ s}^{-1}$.

As in the two-body case, we can write

$$\begin{aligned}
 \Phi(\vec{r}) &= \Psi^2 + \int \frac{d^3\vec{k}}{(2\pi)^3} (C_{\vec{k}}^{ad} + C_{\vec{k}}^{dyn}) \varphi_{\vec{k}}(\vec{r}) \\
 \Phi_m(\vec{r}) &= \Psi_m \varphi_m(\vec{r}),
 \end{aligned}$$

where the adiabatic part $C_{\vec{k}}^{ad} = -\frac{1}{E_{\vec{k}}}(w_{\vec{k}}\Psi_m + g_{\vec{k}}\Psi^2)$ and $g_{\vec{k}} = \langle 0|U|\varphi_{\vec{k}}\rangle$, $|0\rangle$ being the zero-momentum plane wave. Elimination of the adiabatic part is now crucial, because it introduces the light shift Δ' but also the coupling constants $w_{\vec{k}}$ and $g_{\vec{k}}$ without resorting to contact interactions [11]. We find

$$i\hbar\dot{\Psi} = \Psi^* \left(g_0\Psi^2 + \int \frac{d^3\vec{k}}{(2\pi)^3} g_{\vec{k}} C_{\vec{k}}^{dyn} + w_0\Psi_m \right) \quad (12)$$

$$i\hbar\dot{\Psi}_m = \left(\Delta - \Delta' - i\frac{\gamma}{2} \right) \Psi_m + \left(w_0\Psi^2 + \int \frac{d^3\vec{k}}{(2\pi)^3} w_{\vec{k}} C_{\vec{k}}^{dyn} \right) \quad (13)$$

$$i\hbar\dot{C}_{\vec{k}}^{dyn} = E_{\vec{k}} C_{\vec{k}}^{dyn} - i\hbar\dot{C}_{\vec{k}}^{ad}. \quad (14)$$

These equations are similar to those of Ref. [9], but contain no ultraviolet divergence. Thus, we can thus safely set $w_{\vec{k}} = w$ and $g_{\vec{k}} = g = 4\pi\hbar^2 a/M$ without any renormalization.

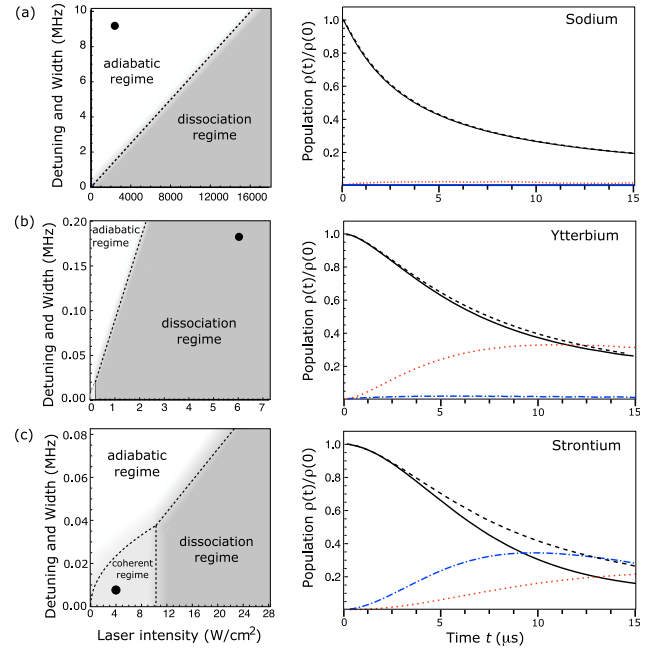


Figure 3: (color online) On-resonance photoassociation ($\Delta - \Delta' = 0$) of a condensate of sodium (a), ytterbium (b) and strontium (c) for typical transitions. In each row, the right panel shows the population evolutions, according to Eqs. (12-14), based on the parameters indicated by the black dot in the left panel, which is a regime diagram similar to Fig. 2. Solid curve: atomic condensate population; dot-dashed curve: molecular population; dotted curve: correlated pair population. The short-dashed curve shows the atomic condensate population following from Eq. (4) with the rate (16). For sodium, we used the conditions of Ref. [12] ($|\text{Im}A|/I = 2.95 \text{ fm}/(\text{Wcm}^{-2})$, $\gamma/\hbar = 18 \text{ MHz}$). Typical intercombination transition parameters were used for ytterbium [22] ($|\text{Im}A|/I = 2.12 \text{ nm}/(\text{Wcm}^{-2})$, $\gamma/\hbar = 364 \text{ kHz}$) and strontium [23] ($|\text{Im}A|/I = 2.12 \text{ nm}/(\text{Wcm}^{-2})$, $\gamma/\hbar = 15 \text{ kHz}$). Thus, we have $(t_w, t_\gamma, t_A) = (0.17, 0.017, 0.0036) \mu\text{s}$ for sodium, $(0.044, 0.88, 35) \mu\text{s}$ for ytterbium, and $(116, 21, 7.8) \mu\text{s}$ for strontium. For all cases, the initial density is $\rho_0 = 6 \cdot 10^{14} \text{ cm}^{-3}$, and $t_\rho \sim 5 \mu\text{s}$.

When the dynamical part $C_{\vec{k}}^{dyn}$ is negligible we obtain the familiar set of coupled Gross-Pitaevskii equations introduced in Ref. [21]. If we assume that $\Psi = \sqrt{\rho_0}$ and $\Psi_m = 0$ initially, these equations admit two limiting regimes [11, 21]. In the adiabatic regime, $w^2\rho_0 \ll (\Delta - \Delta')^2 + (\gamma/2)^2$, the molecular wave function can be adiabatically eliminated, and the condensate density $\rho = |\Psi|^2$ then follows Eq. (4) with the rate coefficient (3) predicted by the stationary two-body theory. On the other hand, in the coherent regime, $w^2\rho_0 \gg (\Delta - \Delta')^2 + (\gamma/2)^2$, Ψ and Ψ_m exhibit coherent Rabi oscillations at a frequency $\Omega = w\sqrt{\rho_0}/\hbar$.

The case where the dynamical part $C_{\vec{k}}^{dyn}$ cannot be neglected corresponds to the “rogue dissociation limit” of Ref. [9]. Ref. [11] showed that this occurs when

$$\rho_0^{1/3}|A| \gg \frac{1}{2} \left(\frac{\pi}{2} \right)^{1/3} \quad \text{and} \quad \rho_0^{1/3}L \gg \frac{1}{2} \left(\frac{\pi}{2} \right)^{1/3} \quad (15)$$

for the adiabatic and coherent regimes, respectively, where

$L = \frac{M}{4\pi\hbar^2} \frac{w}{\sqrt{2\rho_0}}$ was identified with a many-body length. Figure 2 shows the three regimes: adiabatic, coherent and rogue dissociation. Most intriguing has been the dependence of the regime boundaries on the density. In particular, increasing the density makes it easier to reach rogue dissociation from the adiabatic regime, but more difficult from the coherent regime, according to Eqs. (15).

In light of the previous two-body analysis, we can now interpret the adiabatic, coherent and rogue regimes in terms of the two-body regimes (a), (b) and (c). Using the same approximations as in the two-body theory, we can reduce the many-body equations (12-14) to a rate equation with a time-dependent coefficient

$$K(t) = \frac{2}{\hbar} \text{Im} \frac{|w|^2 + gS(t)}{\Delta - \Delta' - i\frac{\gamma}{2} + S(t) - \frac{i\hbar}{t}}. \quad (16)$$

We emphasize that this rate coefficient does not depend on the density and originates essentially from the time-dependent two-body coefficient (7). It follows that the three regimes (a), (b) and (c) also apply for (16). In fact, the conditions for the observation of regime (a), (b) or (c) during the depletion time t_ρ , expressed in terms of t_w , t_γ , and t_A are equivalent to the boundary conditions for respectively the coherent, rogue dissociation, and adiabatic regime, as shown in Fig. 2. Thus, the density dependence of these boundaries originates simply from the usual rate equation of kinetic theory. Note in particular that the rogue regime boundaries (15) are equivalent to the conditions (11) for the observation of the universal regime (b). This shows that the length L has in fact no special significance.

The right panels of Fig. 3 compare the atomic condensate evolution from Eqs. (12-14) with that following from the rate coefficient Eq. (16) in the three regimes. It shows that the short-time evolution is always consistent with two-body dynamics and kinetic theory, justifying the approximations we have made. Only in the coherent regime, for $t \gtrsim t_\rho$, is the condensate nature of the gas revealed due to collective effects which cannot be described by a rate equation.

For alkali-metal atoms experimentally studied in [12, 15], the molecular state has a short lifetime on the order of 10 ns. As a result, these experiments have been confined to the adiabatic regime. Figure 3a shows a typical case for sodium. To reach other regimes, very large intensities are needed. On the other hand, photoassociation near narrow intercombination lines leads to much longer-lived molecules. Figures 3b and 3c show on-resonance photoassociation in condensates of ytterbium and strontium, for typical states below the intercom-

bination line. For moderate intensities, it appears possible to reach the universal regime (b) of pair dissociation. This creates correlated pairs of atoms from a condensate, analogous to correlated photons [24]. For strontium, it should be possible to reach the coherent regime, at least partially. Note, however, that inelastic collisions, while not significantly affecting the atomic condensate, reduce the molecular and non-condensate populations by about a half in Fig. 3c.

In summary, we showed how different regimes of photoassociation in a BEC originate from transient shifts and broadenings in the two-atom dynamics. These have simple analytical expressions, and lead to a universal behavior in the rogue/pair dissociation regime.

We thank the Office of Naval Research for partial support.

-
- [1] T. Köhler, K. Góral, and P. S. Julienne, *Rev. Mod. Phys.* **78**, 1311 (2006).
 - [2] K. M. Jones et al., *Rev. Mod. Phys.* **78**, 483 (2006).
 - [3] D. Meiser, P. Meystre, and C. P. Search, *Phys. Rev. A* **71**, 033621 (2005).
 - [4] T. Kinoshita, T. Wenger, and D. S. Weiss, *Phys. Rev. Lett.* **95**, 190406 (2005).
 - [5] G. B. Partridge et al., *Phys. Rev. Lett.* **95**, 020404 (2005).
 - [6] D. J. Heinzen et al., *Phys. Rev. Lett.* **84**, 5029 (2000).
 - [7] M. Koštrun et al., *Phys. Rev. A* **62**, 063616 (2000).
 - [8] O. Dannenberg and M. Mackie, *Phys. Rev. A* **74**, 053601 (2006).
 - [9] J. Javanainen and M. Mackie, *Phys. Rev. Lett.* **88**, 090403 (2002).
 - [10] T. Gasenzer, *Phys. Rev. A* **70**, 021603(R) (2004).
 - [11] P. Naidon and F. Masnou-Seeuws, *Phys. Rev. A* **73**, 043611 (2006).
 - [12] C. McKenzie et al., *Phys. Rev. Lett.* **88**, 120403 (2002).
 - [13] I. D. Prodan et al., *Phys. Rev. Lett.* **91**, 080402 (2003).
 - [14] M. Theis et al., *Phys. Rev. Lett.* **93**, 123001 (2004).
 - [15] K. Winkler et al., *Phys. Rev. Lett.* **95**, 063202 (2005).
 - [16] J. L. Bohn and P. S. Julienne, *Phys. Rev. A* **60**, 414 (1999).
 - [17] P. O. Fedichev et al., *Phys. Rev. Lett.* **77**, 2913 (1996).
 - [18] T. Köhler and K. Burnett, *Phys. Rev. A* **65**, 033601 (2002).
 - [19] M. Holland, J. Park, and R. Walser, *Phys. Rev. Lett.* **86**, 1915 (2001).
 - [20] V. A. Yurovsky and A. Ben-Reuven, *Phys. Rev. A* **67**, 043611 (2003).
 - [21] E. Timmermans et al., *Phys. Rep.* **315** (1999).
 - [22] S. Tojo et al., *Phys. Rev. Lett.* **96**, 153201 (2006).
 - [23] T. Zelevinsky et al., *Phys. Rev. Lett.* **96**, 203201 (2006).
 - [24] T. Opatrný and G. Kurizki, *Phys. Rev. Lett.* **86**, 3180 (2001).